
Significance of a Single-Time-Point Somatostatin Receptor SPECT/Multiphase CT Protocol in the Diagnostic Work-up of Gastroenteropancreatic Neuroendocrine Neoplasms

Juri Ruf^{1,2}, Friederike von Wedel¹, Christian Furth¹, Timm Denecke³, Lars Stelter³, Ingo G. Steffen¹, Kerstin Schütte⁴, Jörg Arend⁵, Gerhard Ulrich¹, Silke Klose⁶, Jan Bornschein⁴, Ivalya Apostolova¹, and Holger Amthauer¹

¹Klinik für Radiologie und Nuklearmedizin, Universitätsklinikum Magdeburg A.ö.R., Magdeburg, Germany; ²Klinik für Nuklearmedizin, Universitätsklinikum Freiburg, Freiburg, Germany; ³Klinik für Strahlenheilkunde, Campus Virchow-Klinikum, Charité-Universitätsmedizin Berlin, Berlin, Germany; ⁴Klinik für Gastroenterologie, Hepatologie und Infektiologie, Universitätsklinikum Magdeburg A.ö.R., Magdeburg, Germany; ⁵Klinik für Allgemein-, Viszeral-, und Gefäßchirurgie, Universitätsklinikum Magdeburg A.ö.R., Magdeburg, Germany; and ⁶Klinik für Nieren- und Hochdruckkrankheiten, Diabetologie, und Endokrinologie, Universitätsklinikum Magdeburg A.ö.R., Magdeburg, Germany

This prospective study compared a 1-d SPECT/CT protocol with the commonly used 3-d protocol for somatostatin receptor scintigraphy in patients with gastroenteropancreatic neuroendocrine neoplasms. Additionally, the influence of SPECT/CT on patient management was evaluated. **Methods:** From October 2011 to October 2012, all gastroenteropancreatic neuroendocrine neoplasm patients undergoing restaging with somatostatin receptor scintigraphy on a modern SPECT/CT device were enrolled in this study. The protocol consisted of planar imaging at 4, 24, and 48 h; low-dose SPECT/CT at 24 and 48 h; diagnostic CT at 24 h using a triple-phase delay after administration of contrast; and diagnostic SPECT/CT at 24 h. All components of the imaging data were reassessed by 3 masked interpreters. The results were compared with a reference standard based on all clinical, imaging, and histopathology follow-up data available (follow-up range, 24–36 mo; mean, 29.9 mo). The reference standard was defined by a study-specific interdisciplinary tumor board that also reassessed treatment decisions. **Results:** Thirty-one patients were eligible for analysis (18 men and 13 women; mean age, 60.4 y). Ten had no imaging signs of disease and remained disease-free during follow-up. Twenty-one had persistent or recurrent disease (82 lesions: 24 in the liver, 21 in the lymph nodes, 16 in bone, 12 in the pancreas, and 9 in other locations). The respective lesion detection rates for interpreters 1, 2, and 3 were 51.9%, 49.4%, and 71.6% for low-dose SPECT/CT at 24 h; 51.9%, 55.6%, and 67.9% for low-dose SPECT/CT at 48 h; 63.0%, 70.4%, and 85.2% for diagnostic CT; and 77.8%, 84.0%, and 88.9% for diagnostic SPECT/CT. Interobserver agreement was moderate for diagnostic SPECT/CT ($\kappa = 0.44$), diagnostic CT ($\kappa = 0.43$), low-dose SPECT/CT at 48 h ($\kappa = 0.61$), and low-dose SPECT/CT at 24 h ($\kappa = 0.55$). For planar imaging, interobserver agreement was fair after 48 h ($\kappa = 0.36$) and 24 h ($\kappa = 0.38$) and moderate after 4 h ($\kappa = 0.42$). Every lesion detectable on planar imaging or low-dose SPECT/CT was also detectable on diagnostic SPECT/CT. The CT and SPECT components of diagnostic SPECT/CT strongly complemented each other, as 34 of 82 lesions (41.4%) were detected on only the CT component or only the SPECT component. Therapeutic

management was influenced by the diagnostic SPECT/CT interpretation in 8 of 31 patients (25.8%). **Conclusion:** The highest detection rates were achieved by diagnostic SPECT/CT. Thus, a more patient-friendly 1-d protocol is feasible. Furthermore, multiphase SPECT/CT affected management in about a quarter of patients.

Key Words: SPECT/CT; somatostatin receptor; scintigraphy; neuroendocrine neoplasm; multiphase CT

J Nucl Med 2016; 57:180–185

DOI: 10.2967/jnumed.115.161117

Neuroendocrine neoplasms (NENs) are a heterogeneous group of rare, often hormonally active neoplasms derived from cells of the neuroendocrine system with varying malignant potential. Most of these tumors are in the gastroenteropancreatic system (1). Frequent overexpression of somatostatin receptors, especially subtypes 2 and 5, allows functional imaging by radiolabeled somatostatin analogs (2) using either conventional somatostatin receptor scintigraphy (SRS) or somatostatin receptor PET (SR PET) (3). Publications on SR PET/CT using the tracer ⁶⁸Ga-DOTATOC have shown the high impact of hybrid imaging on NEN patient management, emphasizing the synergistic nature of combined functional and anatomic imaging (4,5).

Although the necessary prospective head-to-head comparisons have not yet been performed for an objective comparison of SR PET and SRS (6), published data indicate the superiority of SR PET for the detection of NEN lesions (7–10). Although SR PET can thus be considered the method of choice for functional NEN imaging, it must be acknowledged that not all institutions have access to a PET or PET/CT system (11). Moreover, difficulties may arise in receiving financial reimbursement for PET tracers, whereas conventional SRS with commercially available ¹¹¹In-labeled DTPA (diethylenetriaminepentaacetic acid)-pentetreotide has been well established for more than 20 y (12) and its reimbursement has been approved by both the European Medicines Agency and the U.S. Food and Drug Administration. In addition, with the advent of modern SPECT/CT scanners that have a multislice CT component, the performance of NEN-appropriate multiphase-CT protocols (13) analogous to SR PET/CT (14) should be possible. Conventional

Received May 19, 2015; revision accepted Nov. 11, 2015.

For correspondence or reprints contact: Holger Amthauer, Klinik für Radiologie und Nuklearmedizin, Universitätsklinikum Magdeburg A.ö.R., Leipziger Strasse 44, 39120 Magdeburg, Germany.

E-mail: holger.amthauer@med.ovgu.de

Published online Nov. 25, 2015.

COPYRIGHT © 2016 by the Society of Nuclear Medicine and Molecular Imaging, Inc.

SRS imaging protocols are often time-consuming and hardware-intensive because multiple acquisition sessions over 2–3 d are required (3,15). We therefore performed the current study to assess whether use of a modern SPECT/CT system can streamline the protocol for patient comfort without compromising the derived information. We also analyzed the impact of multiphase SPECT/CT on patient management in comparison to a conventional SRS protocol including low-dose SPECT/CT.

MATERIALS AND METHODS

Patients

Patients with proven low- to intermediate-grade (grade 1 or 2) gastroenteropancreatic NENs undergoing restaging between October 2011 and October 2012 were consecutively enrolled in this prospective, single-center study. Patients were excluded if they had secondary malignancies or an allergy to iodine-containing contrast agents, if they had undergone a contrast-enhanced CT scan within the previous month, or if they were younger than 18 y, pregnant, or breast-feeding. If applicable, long-acting somatostatin analogs were withdrawn at least 4 wk before examination and short-acting analogs at least 24 h before examination (3). The institutional review board approved the study (vote, 96/11), and all subjects gave written informed consent to the examination and to the evaluation of their data. The study was performed in accordance with the Declaration of Helsinki.

Imaging Protocol

All examinations, including contrast-enhanced CT, were performed on a dedicated 16-slice SPECT/CT system (Discovery NM/CT670; GE Healthcare) after intravenous injection of 200 MBq (5.4 mCi) of ¹¹¹In-octreotide (Octreoscan; Mallinckrodt Medical GmbH). SRS was performed in accordance with current guidelines (3,15).

Planar Imaging. Whole-body planar imaging was performed 4, 24, and 48 h after injection. Images were acquired in step-and-shoot mode using medium-energy general-purpose collimators and energy windows centered on $171\% \pm 10\%$ and $245\% \pm 10\%$ ($256 \times 1,024$ matrix, table speed of 13.3 cm/min, and zoom of 1.0).

Low-Dose SPECT/CT. Whole-body low-dose SPECT/CT was performed 24 and 48 h after injection using the same collimators and energy windows as for planar imaging (360° , 60 frames, 40 s per frame, step-and-shoot mode, 6° angles, 128×128 matrix, 540×400 field of view, 2 bed positions, and roughly 4 cm of overlap). The SPECT data were reconstructed iteratively (ordered-subset expectation maximization, 2 iterations, 10 subsets) with CT-based attenuation correction using the low-dose CT images (10 mA, 120 kV, 3.75-mm slice thickness) for generation of the μ -map.

Diagnostic CT and Diagnostic SPECT/CT. Diagnostic CT was performed 24 h after injection using a multiphase delay after administration of intravenous contrast medium (70–100 mL of Imeron 300 [weight-dependent]; Bracco Imaging Deutschland GmbH). The delay was 25 s for the arterial phase and 45 s for the portal-venous phase (upper-abdominal imaging), and there was a 70-s delay for the venous phase (thoracoabdominopelvic imaging) (50–300 mAs as modified by body region and automatic dose modulation [AutomA]; 120 kVp; 16×1.25 mm collimation; pitch of 1.375; and 16×1.25 mm slice thickness). The protocol did not include oral contrast medium.

A dedicated Xeleris workstation (GE Healthcare) was used to co-register the low-dose SPECT/CT images at 24 h with the venous CT images to create the diagnostic SPECT/CT dataset. In evaluating the diagnostic SPECT/CT images, the interpreters also viewed and co-registered the arterial and portal-venous CT images if necessary.

Treatment Decisions

After nonmasked interpretation of the images by radiology and nuclear medicine physicians and review of all imaging, clinical, and para-

clinical data, the patient's case was discussed by the institutional NEN tumor board, which was also responsible for initiating any therapeutic measures deemed necessary.

Masked Data Interpretation

After completion of all follow-up imaging, 3 masked interpreters reassessed the SRS SPECT/CT data (i.e., planar images 4, 24, and 48 h after injection; low-dose SPECT/CT at 24 h; low-dose SPECT/CT at 48 h; diagnostic CT; and diagnostic SPECT/CT) for NEN manifestations. Although the planar images obtained at each time point (4, 24, and 48 h after injection) were interpreted separately, planar imaging as a whole was judged positive if a focus was classified as a lesion on the images of at least one time point.

Each interpreter had long-standing proficiency in hybrid imaging. Data were interpreted in accord with published criteria for SR PET/CT (14). Interpretation was done in random order using a dedicated multimodality workstation. In addition to the individual interpretations, a consensus was reached by the 3 interpreters (majority decision).

Study-Specific Interdisciplinary NEN Tumor Board

The independent study-specific NEN tumor board consisted of a gastroenterologist, nuclear medicine specialist, radiologist, abdominal surgeon, and endocrinologist. Decisions were made in consensus.

This study-specific board served two purposes: to establish a reference standard for the masked-interpretation results based on all clinical and imaging follow-up (follow-up range, 24–36 mo; mean, 29.9 mo) and any available histopathologic or cytologic data, and to use that reference standard to confirm the treatment decisions that had been made by the institutional NEN tumor board.

Statistical Analyses

Statistical analyses were performed using R, version 3.0.1 (The R Foundation for Statistical Computing), and SAS, version 9.3 (SAS Institute Inc.).

Sample Size Estimation. Initially, the necessary sample size was calculated by assuming a 15% clinically relevant difference in lesion-based detection rate. Thus, the 1-sided McNemar power analysis indicated that 60 lesions would be needed for a power of 80% and a significance level of 0.05. Assuming a mean of 2 lesions per patient and a dropout rate of 10%, the total number of patients needed for enrollment was 33.

Data Analysis. Lesions were assessed by each interpreter individually and by all three in consensus. Because of the unavoidable limitations of the established reference standard, the true number of false-negatives is not known. Hence, the term *detection rate* for lesion assessment was chosen. Detection rates were described by 2-sided binomial 95% confidence intervals and analyzed using the generalized linear mixed model, including patients and corresponding lesions as random factor and methods as fixed factor.

Interobserver agreement was calculated using Fleiss κ , which was interpreted according to the classification of Landis and Koch (16). Confidence about the anatomic location of the detected lesions was scored using a binary system (0 = unsure, 1 = sure). To demonstrate the impact of the submodality on interpreter confidence, only lesions seen in all submodalities were included in this analysis.

RESULTS

Patients

Within the 12-mo recruitment period, the required 33 patients were enrolled. Because 1 patient was lost to follow-up and 1 patient had an incomplete set of data, 31 patients were analyzed (18 men and 13 women; mean age, 60.4 y; Table 1).

By the reference standard, the primary was ileum in 10 patients, jejunum in 3, pancreas in 8, duodenum in 2, colon in 1, appendix in 3, rectum in 2, and stomach in 1. In only a single patient did the primary remain unknown. In 21 patients (67.7%), the SPECT/CT examination as a whole was positive for tumor. The remaining 10 patients (32.3%) showed no NENs on SPECT/CT, as was then confirmed by the study-specific NEN tumor board.

Lesion-Based Analysis

In the 21 patients for whom SPECT/CT was positive for tumor, 82 lesions were detected (24 in liver, 21 in lymph nodes, 16 in

bone, 12 in pancreas, and 9 in other locations; mean per patient, 3.9 lesions; range, 1–13).

The respective lesion detection rates for interpreters 1, 2, and 3 and the majority interpretation were 27.2%, 24.7%, 23.5%, and 22.2% for planar scintigraphy (all time points); 51.9%, 49.4%, 71.6%, and 54.3% for low-dose SPECT/CT at 24 h; 51.9%, 55.6%, 67.9%, and 55.6% for low-dose SPECT/CT at 48 h; 63.0%, 70.4%, 85.2%, and 71.6% for diagnostic CT; and—the highest detection rate—77.8%, 84.0%, 88.9%, and 86.4% for diagnostic SPECT/CT (Table 2). Diagnostic SPECT/CT also showed the highest detection rate in the organ-based analysis, particularly with respect to

TABLE 1
Patient Data and Impact on Therapy Management

Patient no.	Sex	Age (y)	Primary location	Grade	Prior therapy	No. of lesions	Change in therapy (confirmed by SITB)
1	M	60.5	Ileum	2	Surgery, octreotide	7	No
2	M	51.2	Rectum	2	Surgery, PRRT	13	No
3	M	39.7	Pancreas	2	Surgery	2	Yes (surgery)
4	F	62.7	Ileum	1	Surgery, octreotide	4	No
5	F	48.5	Ileum	2	Surgery	1	Yes (octreotide, bisphosphonates)
6	M	65.4	Pancreas	1	Surgery	0	No
7	M	46.0	Pancreas	2	Surgery, octreotide	2	No
8	M	51.2	Ileum	2	Surgery	0	No
9	F	73.2	Ileum	2	Surgery, octreotide	2	No
10	F	53.7	Colon	1	Surgery	1	Yes (octreotide, bisphosphonates)
11	F	47.7	Rectum	2	Surgery	2	Yes (surgery)
12	M	67.5	Ileum	2	Surgery, octreotide	8	No
13	M	74.4	Duodenum	2	Surgery	0	No
14	F	55.2	Appendix	1	Surgery	0	No
15	F	76.5	Jejunum	1	Surgery	3	Yes (surgery/ablative therapy)
16	F	60.4	Ileum	1	Surgery	0	No
17	M	59.6	Ileum	2	Surgery	0	No
18	M	70.9	Jejunum	1	Surgery, octreotide	2	No
19	M	54.5	Pancreas	2	Surgery	1	No
20	M	63.3	Stomach	1	Surgery	1	Yes (octreotide)
21	F	61.2	Ileum	2	Surgery, octreotide	2	No
22	F	72.5	Ileum	2	Surgery	0	No
23	M	54.0	Pancreas	2	Chemotherapy	4	No
24	M	67.7	Unknown	2	Octreotide	6	No
25	F	44.2	Appendix	2	Surgery	0	No
26	M	74.8	Duodenum	1	Surgery, octreotide	6	No
27	M	65.7	Pancreas	2	Surgery	2	Yes (surgery)
28	F	56.8	Pancreas	2	Surgery	7	Yes (chemotherapy)
29	F	52.3	Pancreas	1	Surgery	0	No
30	M	57.8	Appendix	1	Surgery	0	No
31	M	82.6	Jejunum	2	Surgery, octreotide	6	No

SITB = study-specific interdisciplinary NEN tumor board; PRRT = peptide-receptor radionuclide therapy.

TABLE 2
Masked-Interpretation Detection Rate According to Interpreter

Interpreter	Planar imaging	Low-dose SPECT/CT		Diagnostic CT	Diagnostic SPECT/CT
		24 h	48 h		
1	27.2 [18.7–37.7]	51.9 [41.1–62.4]	51.9 [41.1–62.4]	63.0 [52.1–72.7]	77.8 [67.6–85.5]
2	24.7 [16.6–35.1]	49.4 [38.8–60.0]	55.6 [44.7–65.9]	70.4 [59.7–79.2]	84.0 [74.5–90.4]
3	23.5 [15.6–33.8]	71.6 [61.0–80.3]	67.9 [57.1–77.1]	85.2 [75.9–91.3]	88.9 [80.2–94.0]
Majority	22.2 [14.5–32.4]	54.3 [43.5–64.7.2]	55.6 [44.7–65.9]	71.6 [61.0–80.3]	86.4 [77.3–92.2]

Data in brackets are 95% confidence intervals.

lesions in liver, bone, and lymph nodes (Table 3). On generalized linear mixed-model analysis, a significantly higher detection rate was found for diagnostic SPECT/CT than for diagnostic CT ($P = 0.013$), for low-dose SPECT/CT at 24 h ($P < 0.001$), or for low-dose SPECT/CT at 48 h ($P < 0.001$). Moreover, every lesion detected on planar imaging or low-dose SPECT/CT and diagnostic CT was also detected on diagnostic SPECT/CT. The CT and SPECT components of diagnostic SPECT/CT strongly complemented each other, as 34 of 82 lesions (41.4%) were detected on only the CT component (22 lesions [26.8%]) or only the SPECT component (12 lesions [14.6%]). Lesions seen on only CT included liver metastases ($n = 9$), lymph node metastases ($n = 8$), lung metastases ($n = 2$), bone metastases ($n = 2$), and pancreatic tumor ($n = 1$). Lesions seen on only SPECT included liver metastases ($n = 4$), lymph node metastases ($n = 3$), bone metastases ($n = 2$), and pancreatic tumor ($n = 3$) (Figs. 1 and 2).

Imaging Time Points

For all interpreters and all time points, planar imaging showed the lowest detection rates (majority rate, 22.2%), with the scan at 4 h having a lower majority rate (14.8%) than the scan at 24 h (21.0%) or 48 h (19.8%). All lesions seen on planar imaging were also seen on low-dose SPECT/CT, which achieved majority rates of 54.3% at 24 h and 55.6% at 48 h (no significant difference between the two time points [$P > 0.05$]). Interpreter 1 had the same detection rate at 24 h as at 48 h (51.9%), interpreter 3 had a higher detection rate at 24 h (71.6%) than at 48 h (67.9%), and interpreter 2 had a lower detection rate at 24 h (49.4%) than at 48 h (55.6%). The highest majority rate, 86.4%, was achieved with diagnostic SPECT/CT. Table 2 summarizes these data.

Interobserver Agreement and Confidence of Anatomic Lesion Assignment

Interobserver agreement (κ value) was moderate for diagnostic SPECT/CT (0.45), diagnostic CT (0.44), and low-dose SPECT/CT at 24 h (0.55) and 48 h (0.61); fair for planar imaging at 24 h (0.38) and 48 h (0.36); and moderate for planar imaging at 4 h (0.42).

Only lesions seen on tomographic imaging were considered in analyzing the confidence of anatomic lesion assignment, because the markedly lower number of lesions seen on planar imaging carried a risk of statistical bias. Confidence was highest for diagnostic SPECT/CT. The respective values for interpreters 1, 2, and 3 were 100%, 100%, and 100% for diagnostic SPECT/CT, followed by 76.7%, 90.3%, and 96.2% for diagnostic CT; 90%, 100%, and 96.2% for low-dose SPECT/CT at 48 h; and 70%, 90.3%, and 86.5% for low-dose SPECT/CT at 24 h.

Impact on Therapeutic Management

The additional lesions detected by diagnostic SPECT/CT, in comparison to the conventional imaging algorithm, had an impact on therapeutic management in 8 of the 31 patients (25.8%) (Table 1). In 13 patients (41.9%), the chosen treatment strategy was not changed. The remaining 10 patients (32.2%) were free of NEN disease and did not undergo any treatment.

Of the 8 patients whose treatment was changed on the basis of the diagnostic SPECT/CT results, 4 patients began receiving systemic therapy: somatostatin analog therapy in 3 patients and chemotherapy (streptozotocin and 5-fluorouracil) in 1 patient (moreover, the additional diagnosis of new bone metastases in 2 patients treated with somatostatin analogs made additional bisphosphonate treatment necessary). In the other 4 patients, local treatment was

TABLE 3
Masked-Interpretation Detection Rate According to Lesion Location

Modality	Liver	Bone	Lymph node	Pancreas	Other
Planar imaging	21.7 [9.7–41.9]	25.0 [10.2–49.5]	9.5 [2.7–28.9]	41.7 [19.3–68]	22.2 [6.3–54.7]
Low-dose SPECT/CT	39.1 [22.2–59.2]	87.5 [64–96.5]	47.6 [28.3–67.6]	75.0 [46.8–91.1]	22.2 [6.3–54.7]
24 h					
48 h	47.8 [29.2–67]	81.2 [57–93.4]	47.6 [28.3–67.6]	75.0 [46.8–91.1]	22.2 [6.3–54.7]
Diagnostic CT	69.6 [49.1–84.4]	87.5 [64–96.5]	76.2 [54.9–89.4]	58.3 [32–80.7]	55.6 [26.7–81.1]
Diagnostic SPECT/CT	87.0 [67.9–95.5]	100.0 [80.6–100]	90.5 [71.1–97.3]	83.3 [55.2–95.3]	55.6 [26.7–81.1]

Data in brackets are 95% confidence intervals.

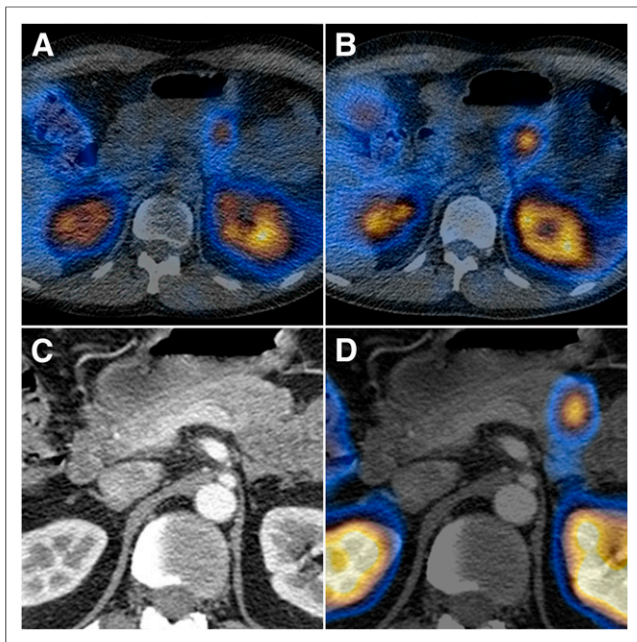


FIGURE 1. Imaging study of 39-y-old man with suspected NEN of pancreas (patient 3 in Table 1). Although focal uptake on low-dose SPECT/CT increased from 24 h (A) to 48 h (B) after injection, focus could be decisively attributed to pancreatic tail only on diagnostic SPECT/CT (D), as contrast-enhanced CT component itself revealed no hypervascularized correlate (C).

indicated: surgery in 3 patients and local ablative therapy (brachytherapy of liver metastases) in 1 patient. All decisions initially made by the institutional NEN tumor board were confirmed in the re-evaluation by the study-specific NEN tumor board.

DISCUSSION

The introduction of SPECT/CT for SRS has been of great value in the anatomic assignment of NEN lesions (17–19) and—because of early implementation of attenuation correction—in the improvement of image quality (20). Not surprisingly, the resulting evolving role of SPECT/CT in the management of NEN tumors has recently been emphasized in a review by Fuccio et al. (21).

A common limitation of NEN imaging studies, including the current study, is the lack of a true histopathologic gold standard for verification of lesions. This is why we chose to use modality performance as a surrogate reference standard, as described by the term *detection rate*. The study-specific NEN tumor board could only inadequately assess the true number of lesions in our patient cohort and the occurrence of false-negative lesions. Despite this limitation, a comparison of the submodalities (e.g., planar imaging vs. low-dose SPECT/CT) within the bounds of our study was still feasible using detection rate as the performance parameter. Our analysis showed that the highest majority detection rate could be achieved when SPECT/CT was combined with diagnostic CT (86.4%), followed by diagnostic CT alone (71.6%) and low-dose SPECT/CT (54.3% at 24 h and 55.6% at 48 h), whereas planar imaging performed the worst (22.2%).

The important role of multiphase CT must be acknowledged. In a comparative study by Rappeport et al. (22), CT detected 16 of 19 lesions (84.2%) and low-dose SPECT/CT 11 of 19 (57.9%). In our study also, the detection rate of diagnostic CT was superior to that

of low-dose SPECT/CT (71.6% vs. 54.3% at 24 h and 55.6% at 48 h; Table 2), with the exception of pancreatic NENs (75% for low-dose SPECT/CT at 24 h vs. 58.3% for diagnostic CT; 83.3% for diagnostic SPECT/CT; Table 3; Fig. 1). Although a direct comparison of the two studies is limited by the differences between them (retrospective vs. prospective, masked vs. nonmasked, dedicated abdominal vs. whole-body imaging, preoperative vs. post-operative examination, many extrapancreatic gastrinoma patients vs. none), the diagnostic value of multiphase CT was confirmed by our study. Another important observation was that lesions were detected to a greater extent (41.4%) by either the nuclear medicine component alone or the radiologic component alone. This was the case in every category of lesion (apart from lung metastases, whose detection on SPECT was limited by, for example, partial-volume effects). Thus, in analogy to PET/CT, the superiority of multiphase SPECT/CT is explained by the complementary nature of the diagnostic CT scan and the SPECT scan, providing the anatomometabolic information needed to choose the therapy for NEN disease (4).

Another similarity to PET/CT imaging is the fact that modern SPECT/CT systems allow whole-body tomographic acquisitions (albeit with longer acquisition times than for PET). In accordance with the reported improved target-to-background ratios for acquisitions at 24 h compared with 48 h (3,15), neither planar nor tomographic imaging at 48 h showed a relevant improvement over imaging at 24 h ($P > 0.05$). However, we believe that the protocol should still include easily obtainable planar acquisitions (at least of distal body parts such as the head and extremities) to obtain a true whole-body examination.

Thus, our data show that with modern SPECT/CT, a streamlined and more patient-friendly SRS examination using ^{111}In -labeled somatostatin receptor ligands at a single time point (planar imaging and SPECT/CT) is feasible, confirming the assumption of

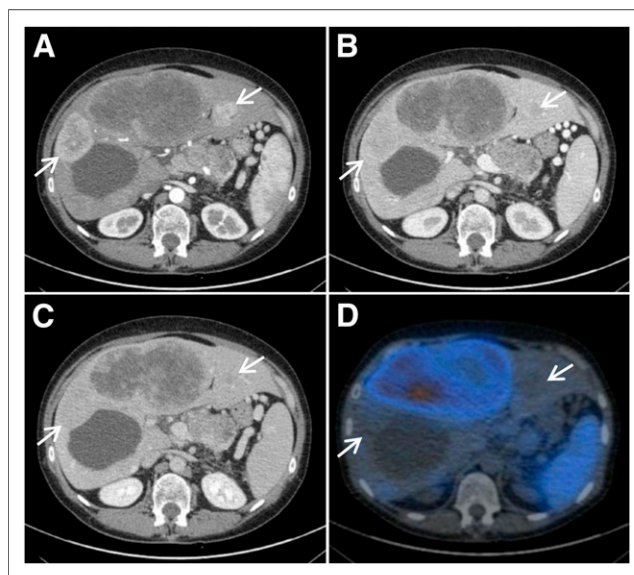


FIGURE 2. Imaging study of 62-y-old woman with NEN of terminal ileum (patient 4 in Table 1). (A) Hepatic metastases in liver segments 5 and 3 (arrows) were clearly visible on CT because of hypervascularization. (B and C) Within portal-venous (B) and venous (C) phases, only slight washout was evident on CT. (D) On SPECT, uptake was observed in central metastasis of segment 4, but no relevant radioligand was taken up in adjacent hyperperfused lateral satellite metastases.

Wong et al. that in SR SPECT/CT an acquisition at 24 h may be sufficient (23). Moreover, SPECT/CT affected therapy management in about 25% of patients by detecting previously unknown lesions, resulting in alteration of the initial treatment strategy. Although this observation is in line with experience with SR PET/CT imaging, the absolute rate of examinations resulting in treatment changes is lower than in PET/CT imaging, which has been reported to alter therapy management in more than half of patients (4,5). This apparent inferiority of SPECT/CT can be explained in part by the poorer performance of conventional SRS than of SR PET (7,8,10). In analogy, and taking such biases as those due to statistics or different patient populations aside, the majority detection rate of conventional SRS, including SPECT, in the present study was only 55.6% (low-dose SPECT/CT at 48 h) and does not compare with the performance of the SR PET component (72.8%) in PET/CT (14).

In this context, it must be mentioned that the performance of SRS may be improved with ^{99m}Tc-labeled SR ligands. In a head-to-head comparison of ^{99m}Tc-labeled hydrazinonicotinyl-Tyr³-octreotide and ¹¹¹In-octreotide, the former showed a higher sensitivity and higher lesional uptake and could be performed as a 1-d examination (24). Moreover, the ^{99m}Tc-based approach is also clearly advantageous with regard to tracer availability and quality of image reconstruction. Therefore, further prospective comparative studies between these two tracers are needed. Finally, even taking the prospect of better SPECT or SPECT/CT performance with ^{99m}Tc-labeled tracers into account, a recent metaanalysis on SR PET and PET/CT reported an impressive sensitivity of 93% and specificity of 91% for the detection of NENs (25). Thus, we believe that SR PET/CT should be the modality of choice for initial staging, before curative surgery, or in patients with an unknown primary. However, in accord with Schillaci et al. (26), we conclude that the detection rate of 86% achieved by modern SR SPECT/CT technique may provide valuable information in a noncurative setting for patients with metastatic disease under systemic therapy if SR PET/CT is not available.

CONCLUSION

With state-of-the-art SPECT/CT scanners, it is possible to streamline the conventional ¹¹¹In-DTPA-octreotide SRS protocol to a single planar and tomographic whole-body acquisition at 24 h after injection. As expected from PET/CT, the integration of a triple-phase CT protocol provided robust results, had the highest NEN lesion detection rate, and greatly improved interpreter confidence in anatomic lesion assignment. Also, similar to SR PET/CT, conventional hybrid imaging by SPECT/CT had a high impact on patient management and therapy planning.

DISCLOSURE

The costs of publication of this article were defrayed in part by the payment of page charges. Therefore, and solely to indicate this fact, this article is hereby marked "advertisement" in accordance with 18 USC section 1734. Mallinckrodt/Covidien cofinanced the trial. No other potential conflict of interest relevant to this article was reported.

ACKNOWLEDGMENTS

We thank Sylvia Hermann, Heike Schmidt, Corinna Herkula, Christel Besseler, and Christian Lössel for their support with patient examinations and data preparation.

REFERENCES

1. Modlin IM, Oberg K, Chung DC, et al. Gastroenteropancreatic neuroendocrine tumours. *Lancet Oncol*. 2008;9:61–72.
2. Fani M, Braun F, Waser B, et al. Unexpected sensitivity of sst2 antagonists to N-terminal radiometal modifications. *J Nucl Med*. 2012;53:1481–1489.
3. Kwekkeboom DJ, Krenning EP, Scheidhauer K, et al. ENETS consensus guidelines for the standards of care in neuroendocrine tumors: somatostatin receptor imaging with ¹¹¹In-pentetreotide. *Neuroendocrinology*. 2009;90:184–189.
4. Ruf J, Heuck F, Schiefer J, et al. Impact of multiphase Ga-68-DOTATOC-PET/CT on therapy management in patients with neuroendocrine tumours. *Neuroendocrinology*. 2010;91:101–109.
5. Frilling A, Sotiropoulos GC, Radtke A, et al. The impact of ⁶⁸Ga-DOTATOC positron emission tomography/computed tomography on the multimodal management of patients with neuroendocrine tumors. *Ann Surg*. 2010;252:850–856.
6. Öberg K. Gallium-68 somatostatin receptor PET/CT: is it time to replace ¹¹¹indium DTPA octreotide for patients with neuroendocrine tumors? *Endocrine*. 2012;42:3–4.
7. Gabriel M, Decristoforo C, Kandler D, et al. ⁶⁸Ga-DOTA-Tyr³-octreotide PET in neuroendocrine tumors: comparison with somatostatin receptor scintigraphy and CT. *J Nucl Med*. 2007;48:508–518.
8. Kowalski J, Henze M, Schuhmacher J, et al. Evaluation of positron emission tomography imaging using [⁶⁸Ga]-DOTA-D Phe¹-Tyr³-octreotide in comparison to [¹¹¹In]-DTPAOC SPECT: first results in patients with neuroendocrine tumors. *Mol Imaging Biol*. 2003;5:42–48.
9. Buchmann I, Henze M, Engelbrecht S, et al. Comparison of ⁶⁸Ga-DOTATOC PET and ¹¹¹In-DTPAOC (Octreoscan) SPECT in patients with neuroendocrine tumours. *Eur J Nucl Med Mol Imaging*. 2007;34:1617–1626.
10. Srirajakanthan R, Kayani I, Quigley AM, Soh J, Caplin ME, Bomanji J. The role of ⁶⁸Ga-DOTATATE PET in patients with neuroendocrine tumors and negative or equivocal findings on ¹¹¹In-DTPA-octreotide scintigraphy. *J Nucl Med*. 2010;51:875–882.
11. Hellwig D, Grgic A, Kotzerke J, Kirsch CM. Nuclear medicine in Germany: key data from official statistics. *Nuklearmedizin*. 2011;50:53–67.
12. Krenning EP, Kwekkeboom DJ, Bakker WH, et al. Somatostatin receptor scintigraphy with [¹¹¹In]-DTPA-D-Phe¹- and [¹²³I]-Tyr³-octreotide: the Rotterdam experience with more than 1000 patients. *Eur J Nucl Med*. 1993;20:716–731.
13. Sundin A, Vullierme MP, Kaltsas G, Plockinger U. ENETS consensus guidelines for the standards of care in neuroendocrine tumors: radiological examinations. *Neuroendocrinology*. 2009;90:167–183.
14. Ruf J, Schiefer J, Furth C, et al. Ga-68-DOTATOC PET/CT imaging of neuroendocrine tumors: spotlight on the CT-phases of a triple-phase-protocol. *J Nucl Med*. 2011;52:697–704.
15. Balon HR, Brown TL, Goldsmith SJ, et al. The SNM practice guideline for somatostatin receptor scintigraphy 2.0. *J Nucl Med Technol*. 2011;39:317–324.
16. Landis JR, Koch GG. The measurement of observer agreement for categorical data. *Biometrics*. 1977;33:159–174.
17. Pfannenberg AC, Eschmann SM, Horger M, et al. Benefit of anatomical-functional image fusion in the diagnostic work-up of neuroendocrine neoplasms. *Eur J Nucl Med Mol Imaging*. 2003;30:835–843.
18. Amthauer H, Ruf J, Bohmig M, et al. Diagnosis of neuroendocrine tumours by retrospective image fusion: is there a benefit? *Eur J Nucl Med Mol Imaging*. 2004;31:342–348.
19. Amthauer H, Denecke T, Rohlfing T, et al. Value of image fusion using single photon emission computed tomography with integrated low dose computed tomography in comparison with a retrospective voxel-based method in neuroendocrine tumours. *Eur Radiol*. 2005;15:1456–1462.
20. Steffen IG, Mehl S, Heuck F, et al. Attenuation correction of somatostatin receptor SPECT by integrated low-dose CT: is there an impact on sensitivity? *Clin Nucl Med*. 2009;34:869–873.
21. Fuccio C, Spinapoliche EG, Chondrogiannis S, et al. Evolving role of SPECT/CT in neuroendocrine tumors management: staging, treatment response, and follow-up. *Clin Nucl Med*. 2013;38:e384.
22. Rappaport ED, Hansen CP, Kjaer A, Knigge U. Multidetector computed tomography and neuroendocrine pancreaticoduodenal tumors. *Acta Radiol*. 2006;47:248–256.
23. Wong KK, Wynn EA, Myles J, Ackermann RJ, Frey KA, Avram AM. Comparison of single time-point [¹¹¹In]-pentetreotide SPECT/CT with dual time-point imaging of neuroendocrine tumors. *Clin Nucl Med*. 2011;36:25–31.
24. Gabriel M, Decristoforo C, Donnemiller E, et al. An inpatient comparison of ^{99m}Tc-EDDA/HYNIC-TOC with ¹¹¹In-DTPA-octreotide for diagnosis of somatostatin receptor-expressing tumors. *J Nucl Med*. 2003;44:708–716.
25. Treglia G, Castaldi P, Rindi G, Giordano A, Rufini V. Diagnostic performance of gallium-68 somatostatin receptor PET and PET/CT in patients with thoracic and gastroenteropancreatic neuroendocrine tumours: a meta-analysis. *Endocrine*. 2012;42:80–87.
26. Schillaci O, Spanu A, Palumbo B, Danieli R. SPECT/CT in neuroendocrine tumours. *Clin Transl Imaging*. 2014;2:477–489.